Modeling of hydrogeochemical processes influencing uranium migration in anthropized arid environments with application to the Teloua aquifer

Laurent de Windt, P. Grizard, C. Besançon, F. Assalack, I. Djibo Hama, P.E. Reiller, N. Seigneur, M. Descostes

Journal of Contaminant Hydrology 269 (2025) 104507

Contents lists available at ScienceDirect

Journal of Contaminant Hydrology

journal homepage: www.elsevier.com/locate/jconhyd

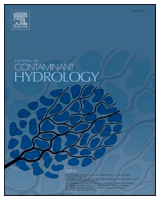

Modeling of hydrogeochemical processes influencing uranium migration in anthropized arid environments with application to the Teloua aquifer

L. De Windt [a,*], P. Grizard [b], C. Besançon [b], F. Assalack [c], I. Djibo Hama [d], P.E. Reiller [e], N. Seigneur [a], M. Descostes [a,b]

[a] Mines Paris, PSL University, Center for Geosciences and Geoengineering, France
[b] ORANO Mining, Environmental R&D Dpt., France
[c] ORANO Mining Niger, Niamey, Niger
[d] COMINAK, Niamey, Niger
[e] Université Paris-Saclay, CEA, Service de Physico-Chimie (SPC), F-91191 Gif-sur-Yvette, CEDEX, France

ARTICLE INFO

Keywords:
Distribution coefficient
HYTEC
Natural attenuation
Teloua aquifer
Uranium mine
Uranyl complex

ABSTRACT

Sandstone-hosted uranium is mined in the Sahel regions of Niger. The Teloua aquifer is located beneath the ore-processing facilities of one such former mine, COMINAK. The pores of the sandstone bedrock are partially filled by tosudite, a clay with sorption capacities. The local groundwater presents a strong oxidizing signature and very low water recharge. This study aims to determine the geochemical baseline of anthropogenic activity for uranium under such extreme conditions. The major and trace elements of both the contaminated and the pristine local groundwaters were sampled and analyzed to develop geochemical and reactive transport models. Kd distribution coefficients were calculated a posteriori from the mechanistic simulations. The entire water chemistry, with large variations in calcium, carbonate and sulfate concentrations, had to be taken into account to properly simulate the speciation and migration of U(VI) in the aquifer locally affected by the mining activities. U(VI) sorption significantly decreases during the propagation of the contaminant plume, due to the formation of $Ca_nUO_2(CO_3)_3^{(4-2n)-}$ complexes that were clearly demonstrated by TRLFS acquisition. The sorption of $UO_2(CO_3)_n^{(2-2n)}$ can play a key role in the immobilization of U(VI). The mitigating factors for U(VI) are sorption on clay and the dispersion/dilution of the contaminated source terms within the groundwater, in which the strong ternary complexes are less important. There should be an efficient immobilization of fixed anthropic uranium by natural attenuation once the contaminant source terms have become depleted.

1. Introduction

During the last few years, the groundwater resources in sub-Saharan / Sahelian regions have been increasingly studied due to their particularly high importance for community water supply (Trabelsi et al., 2024; Zouari et al., 2024). The review of Edmunds (2003) indicates that the local aquifers of the arid and semi-arid sub-Saharan regions present a strong oxidizing signature. These aquifers are characterized by relatively high concentrations of redox-sensitive metals (e.g. Cr, Mo) and metalloids (e.g. As), as well as long lifetimes of dissolved oxygen O_2 (up to 20,000 years) and nitrate NO_3^-. The recharge of this type of aquifer was mostly generated by paleo-recharges, and the present-day Darcy flowrates are less than 1 m/year. These very low rainwater recharges combined with low organic-matter content prevent any significant reducing microbial activity.

The Sahel regions are also significant for the mining of uranium deposits which are hosted in the local sandstone (see Mamadou et al., 2022 and references therein). Therefore, determining the baseline of any anthropogenic activities for uranium is a key issue in the Sahelian oxidizing aquifers. Many aquifers elsewhere in the world are under reducing conditions and uranium is usually considered as immobile under its insoluble U(IV) redox state (Finch and Murakami, 1999). However, uranium in its U(VI) redox state is relatively soluble (Finch and Murakami, 1999) and, therefore, possibly mobile in aquifers. The persistence of oxidizing conditions implies that the cation uranyl UO_2^{2+} and its numerous aqueous complexes are expected to remain stable for a very long time. For instance, Burow et al. (2017) recently found a strong positive correlation between mobile U(VI) and bicarbonate (HCO_3^-)

* Corresponding author.
E-mail address: laurent.de_windt@minesparis.psl.eu (L. De Windt).

https://doi.org/10.1016/j.jconhyd.2025.104507
Received 28 October 2024; Received in revised form 24 December 2024; Accepted 19 January 2025
Available online 20 January 2025

concentrations in irrigated waters from the arid zones of western USA, although they did not measure any relationship in wetlands where oxygen rapidly disappears and favors the reduction of uranium to the less mobile U(IV) form.

In Niger, the COMINAK uranium mine opened in 1978 and ceased production after nearly 50 years and a total production of approximately 75,000 tU. The mine is currently under remediation for a period of 10 years (Ascani, 2021). The extracted uranium deposits originated from the Tim Mersoï sedimentary basin, located in the Arlit region of the Sahel desert. The climate is extremely arid with an annual mean temperature of 31 °C and an annual precipitation of about 40 mm (Dodo and Zuppi, 1999). The Teloua aquifer outcrops in the western section of the mining site, which raises the possibility of uranium contamination and migration. During both the production and remediation phases of the COMINAK mine, the water quality of each aquifer potentially affected by mining activities has been monitored. This monitoring has revealed the presence of very localized chemical markers (sulfate and uranium) in the Teloua aquifer while maintaining neutral pH conditions. Remediation operations are currently in place to contain this contamination and treat the water. Understanding the hydrogeochemical behavior of dissolved uranium is a crucial element in the strategy for managing impacted water.

In this context, the present study aims to model the possible migration of uranium in the Teloua aquifer by highlighting the importance of the groundwater chemistry (major elements) and the minerals participating in its regulation (clays). The first input of the study is to provide for relatively scarce field data on the hydrochemistry of anthropized mining areas in an arid climate. Field sampling, chemical analysis and time-resolved laser fluorescence spectroscopy (TRLFS) were performed for both the pristine Teloua groundwater and locally contaminated waters. The measurement of major (Ca^{2+}, SO_4^{2-}…) and trace elements (U, As, Mo…) allows to relate uranium concentrations to information on their chemical environment.

The second input is to develop two mechanistic models based on these waters and Teloua bedrock data previously acquired in the zones located downstream from the mine (Abd Elmola et al., 2020). The lack of sorption experiment is partly overcome by using surface complexation constants from the literature. The geochemical model quantifies the competition between U(VI) sorption on the Teloua bedrock and U(VI) complexation in the porewater depending on ternary $(Mg,Ca)_nUO_2(CO_3)_3^{(4-2n)-}$ complexes. The reactive transport model simulates the long-term migration of the contaminated plume for different scenarios. This model is not an environmental assessment of the COMINAK mine but rather aims to provide helpful insights on possible key reactive transport mechanisms. In particular, the immobilization of uranium by natural attenuation is analyzed by modeling.

In a last step, distribution coefficients (Kds) are calculated a posteriori from the geochemical and reactive transport mechanistic simulations. These Kds can then be used as reference values for non-reactive transport codes, as indicators of the local disturbance of the geochemical properties and for comparison with Kd data from the literature.

2. Experimental and modeling methods

2.1. Water sampling and analysis

2.1.1. On-site water sampling

Three boreholes drilled by COMINAK were sampled. One borehole was located about 2.5 km downstream from the mine perimeter to the west of the Arlit fault: this gave access to pristine Teloua water. The two other boreholes were drilled into contaminated groundwater streams.

Compact submersible pumps (Grundfos, SQ3) were used to sample groundwater from the boreholes after an initial draining. The pH was simply measured in situ with a pH-meter (Hanna HI 9828). The water samples were collected and filtered at 0.45 μm for major, uranium, and trace element analysis. The samples for anion analysis were unacidified while the others were acidified with ultrapure nitric acid.

2.1.2. Chemical analysis

The pH values were also measured in the lab by electrochemistry (NF EN ISO 10523). Major cations were analyzed by inductively coupled plasma atomic emission spectrometry (ICP-AES) (NF EN ISO 11885), chloride/fluoride/sulfate by ionic chromatography (IC) (NF EN ISO 10304-1), silicate/nitrate by continuous flow analysis (CFA) (NF EN ISO 13395), bicarbonate/carbonate by potentiometric titration (NF EN 9963–1), and uranium and trace elements by inductively coupled plasma mass spectrometry (ICP-MS) (NF EN ISO 17294-1-2).

2.1.3. TRLFS acquisition

The apparatus for time-resolved laser-induced fluorescence spectroscopy (TRLFS) has been extensively described in previous works (Shang and Reiller, 2020). It consisted of an Nd-YAG pulsed laser (Surelite II, Continuum, USA) delivering 5 ns pulses of 170 mJ energy at 10 Hz. An optical parametric oscillator (OPO, Horizon, Continuum, USA) adjusted the selective U(VI) excitation wavelength to 450 nm (around 20 mJ) to give the best compromise between U(VI) fluorescence yield and OPO efficiency. The luminescence was collected at 90° to the incident beam and focused on the entrance slit of an ANDOR spectrometer (300 lines/mm grating). Luminescence spectra were acquired at a delay D after the laser pulse during a digital gate width W of 1 μs.

2.2. Modeling approach and database

2.2.1. Geochemical and reactive transport modeling

The HYTEC reactive transport code (van der Lee et al., 2002; van der Lee et al., 2003) was used for modeling the speciation and migration of U in the impacted Teloua aquifer. HYTEC has been recently used in the modeling of several mining environmental issues such as acid mine drainage (Garcia-Rios et al., 2021), mine tailing containment (Seigneur et al., 2021), and in-situ leaching remediation (Lagneau et al., 2019; de Boissezon et al., 2020; Escario et al., 2023).

The formula for multicomponent reactive transport in HYTEC is the following,

$$\frac{\partial \omega [C_i]}{\partial t} = div\,(D_d\, grad\,[C_i] - [C_i]\,\boldsymbol{U}) - \frac{\partial \omega\, \overline{[C_i]}}{\partial t} \quad (1)$$

where $[C_i]$ is the total mobile (i.e. dissolved in porewater) concentration of an element or species i (basis component approach) per unit volume of porewater, $\overline{[C_i]}$ is the immobile (i.e. sorbed or mineral) concentration of the element/species i (also expressed per unit volume of porewater, for consistency), ω is the porosity, D_d is the effective diffusion/dispersion coefficient and U is the Darcy velocity. The volume of porewater is equal to the pore volume under full water-saturated conditions. The term $\frac{\partial \omega\, \overline{[C_i]}}{\partial t}$ is driven by the chemical reactions whereas the other terms are linked to the transport processes. Chemistry and transport are coupled through a sequential iterative algorithm.

All chemical reactions (aqueous chemistry, sorption and dissolution/precipitation of minerals) were modeled at thermodynamic equilibrium with the PRODATA thermodynamic database, version 1.5.2 (Reiller and Descostes, 2020), specifically developed for mining activities and environmental monitoring. Due to their importance for the present study, Table 1 provides the thermodynamic formation constants of the ternary

Table 1
Thermodynamic formation constants of the ternary complexes $Ca_nUO_2(CO_3)_3^{(4-2n)-}$ included in the model (Shang and Reiller, 2020; Shang and Reiller, 2021).

Reaction of complexation	logK (25 °C)
$UO_2^{2+} + Ca^{2+} + 3\,CO_3^{2-} \rightleftharpoons CaUO_2(CO_3)_3^{2-}$	27.2
$UO_2^{2+} + 2\,Ca^{2+} + 3\,CO_3^{2-} \rightleftharpoons Ca_2UO_2(CO_3)_3$	30.5
$UO_2^{2+} + Mg^{2+} + 3\,CO_3^{2-} \rightleftharpoons MgUO_2(CO_3)_3^{2-}$	26.4

complexes $Ca_nUO_2(CO_3)_3^{(4-2n)-}$ included in the model. These latter complexes were recently shown to be particularly sensitive to an ionic strength higher than 0.1 M (Shang and Reiller, 2020; Reiller, 2024). As the majority of the sampled water was lower than 0.2 M, for the sake of simplicity, activity corrections were calculated with the truncated Davies model applicable for low to moderate ionic strength.

2.2.2. Modeling of sorption by cation exchange and surface complexation

The PRODATA database was supplemented with data from well-validated sorption reactions on montmorillonite from the literature (Table 2). As discussed in Section 3.1.2, the sorption properties of the Teloua bedrock can be attributed to the tosudite clay that consists of chlorite and montmorillonite end-members. Only cation-exchange capacities of the Teloua sandstone were determined. As a reasonably good approximation, cation exchange and surface complexation of tosudite were modeled by the well-known set of constants of montmorillonite from the literature (Table 2).

Cation exchange between the major ions (Na^+, K^+, Mg^{2+}, Ca^{2+}) as well as UO_2^{2+} was modeled via the Gaines-Thomas convention. Surface complexation on the montmorillonite surface was modeled by a non-electrostatic model. These data include sorption of UO_2^{2+}, as well as of certain hydroxyl complexes (e.g. UO_2OH^+) and carbonate complexes (e.g. UO_2CO_3) that play an important role with respect to the present chemistry of the contaminated plume.

The empirical coefficient Kd expressed in L/kg is the ratio between the total concentration of U(VI) sorbed per kg of solid [S] (i.e. the Teloua bedrock here) to the total concentration of U(VI) in solution [C] (i.e. in Teloua porewater here):

$$K_d = \frac{[S]}{[C]} \text{ in } \left[\frac{mol/kg_{bedrock}}{mol/L_{porewater}}\right] \quad (2)$$

The final results of the geochemical and reactive transport modeling were used to calculate the Kd values of U(VI) a posteriori (i.e. not as initial parameters of the transport modeling), to give reference values for the pristine and impacted Teloua aquifer.

Table 2
Cation exchange and surface complexation constants included in the model.

Reactions of sorption	logK (25 °C)	Ref.
Cation exchange (Gaines-Thomas model)		
$\overline{Na^+} + K^+ \rightleftharpoons \overline{K^+} + Na^+$	0.60	[a]
$2\,\overline{Na^+} + Ca^{2+} \rightleftharpoons \overline{Ca^{2+}} + 2\,Na^+$	0.41	[a]
$2\,\overline{Na^+} + Mg^{2+} \rightleftharpoons \overline{Mg^{2+}} + 2\,Na^+$	0.34	[a]
$2\,\overline{Na^+} + UO_2^{2+} \rightleftharpoons \overline{UO_2^{2+}} + 2\,Na^+$	0.45	[b]
Surface complexation (non-electrostatic model)		
$\equiv S^sOH \rightleftharpoons \equiv S^sO^- + H^+$	−7.9	[c]
$\equiv S^sOH + H^+ \rightleftharpoons \equiv S^sOH_2^+$	4.5	[c]
$\equiv S^wOH \rightleftharpoons \equiv S^wO^- + H^+$	−7.9	[c]
$\equiv S^wOH + H^+ \rightleftharpoons \equiv S^wOH_2^+$	4.5	[c]
$\equiv S^sOH + UO_2^{2+} \rightleftharpoons \equiv S^sUO_2^+ + H^+$	3.1	[b]
$\equiv S^sOH + UO_2^{2+} + H_2O \rightleftharpoons \equiv S^sUO_2OH + 2\,H^+$	−4.6	[b]
$\equiv S^sOH + UO_2^{2+} + 2\,H_2O \rightleftharpoons \equiv S^sUO_2(OH)_2^- + 3\,H^+$	−12.6	[b]
$\equiv S^sOH + UO_2^{2+} + 3\,H_2O \rightleftharpoons \equiv S^sUO_2(OH)_3^{2-} + 4\,H^+$	−20.9	[b]
$\equiv S^wOH + UO_2^{2+} \rightleftharpoons \equiv S^wUO_2^+ + H^+$	0.5	[b]
$\equiv S^wOH + UO_2^{2+} + H_2O \rightleftharpoons \equiv S^wUO_2OH + 2\,H^+$	−5.7	[b]
$\equiv S^sOH + UO_2^{2+} + 1\,CO_3^{2-} \rightleftharpoons \equiv S^sUO_2CO_3^- + H^+$	9.8	[b]
$\equiv S^sOH + UO_2^{2+} + 2\,CO_3^{2-} \rightleftharpoons \equiv S^sUO_2(CO_3)_2^{3-} + H^+$	15.5	[b]
$\equiv S^wOH + UO_2^{2+} + 1\,CO_3^{2-} \rightleftharpoons \equiv S^wUO_2CO_3^- + H^+$	9.3	[b]

[a] Bradbury and Baeyens (2003); [b] Marques Fernandes et al. (2012); [c] Bradbury and Baeyens (1997).

3. Background geochemistry and contaminant source term

3.1. Properties of the Teloua aquifer

3.1.1. Geological configuration

The sandstone Teloua Formation is part of the Tim Mersoï Basin located in northeast Niger (Andrews et al., 1994). This formation, which is cut by the major Arlit Fault, is about 70 m thick and outcrops only in the western section of the COMINAK mining site, a few hundred meters from the Arlit Fault to the west (Fig. 1). The formation dips predominantly from north to south at around 0.43°. From west to east, at the level of the Fault, the geological layers reach an average slope of around 35° over 1 km of flexure. The slope quickly levels out, and the aquifer then flows a nearly horizontal direction at a depth of about 100 to 150 m / floor.

3.1.2. Mineralogical and petrophysical properties

The mineralogical properties of the Teloua bedrock extracted from the selected boreholes are sourced from an existing study (Abd Elmola et al., 2020). This porous sandstone mainly consists of quartz grains (> 85 wt%) and alkali feldspars (albite, microcline), whose inter-grain porosity is partially filled by tosudite (Table 3). Tosudite is an authigenic interlayered clay phase with sorption properties. The two end members of tosudite are sudoite (di-trioctahedral chlorite, about 70 mol %) and montmorillonite (dioctahedral smectite, about 30 mol%). Heavy minerals such as iron oxides (hematite), phosphates (apatite and monazite), and titanium oxides (anatase) are also present in small proportions. Only a very few grains of apatite containing uranium were observed, calcite is only present at trace levels, and there is no organic matter. The mean measured content of uranium in the solid phase was 1.3 ppm. No uranium minerals could be explicitly identified.

In addition, cation exchange capacities (CEC) were measured on several samples from each borehole, both on the clay fraction and on the total rock. The results confirmed the reactivity of the clay minerals, i.e. their accessibility to fluids, with CEC values between 50 and 60 meq/100 g for the fine fraction and between 2.9 and 5.2 meq/100 g for the total rock. The CEC of pure tosudite is about 50 meq/100 g (Brown et al., 1974). The CEC of the Teloua bedrock is relatively low compared with clayey sedimentary rocks but it can, nevertheless, play a role in the regulation of the chemistry and U sorption.

The density of the dried bedrock was set at 2.2 kg/dm^3. The total porosity decreases with increasing depth as a result of grain compaction and the development of authigenic clay minerals that cemented the pore spaces. The effective porosity for modeling migration was set at 0.08 and assumed to be fully saturated with water.

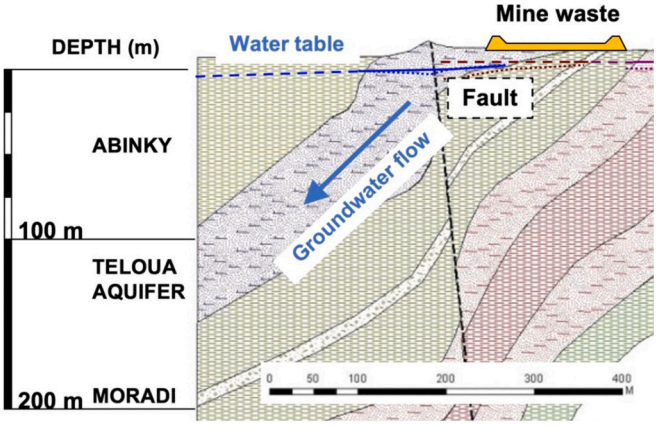

Fig. 1. Diagram of the Teloua aquifer flowing between the Abinky and Moradi aquitards, showing the 1D modeling flow line downstream from the main local fault and the mine waste facility.

Table 3
Mineralogy of the Teloua aquifer sandstone.

Mineralogy	Mean values
Quartz	86.5 wt%
Na/K - Feldspars	8 wt%
Tosudite (clay)	5 wt%
Hematite	0.5 wt%
Calcite	Trace level (0.1 wt%)

3.1.3. Groundwater chemistry

Table 4 gives the groundwater chemistry of the Teloua aquifer, both for the major and the trace elements, determined in the present study. For the sake of clarity, 'groundwater' will refer to the water of the Teloua aquifer in its natural, 'pristine' state (natural chemical background) whereas 'porewater' will be used for the contaminated water in the affected aquifer. The groundwater is poorly mineralized, has a sodic bicarbonate facies, a neutral pH and is moderately oxidizing. It can be considered of high quality since all its chemical parameters are substantially below the potability thresholds of the World Health Organization's (WHO) guidelines.

Table 5 gives the calculated saturation indices (SI) of the main minerals of the bedrock as well as of common uranyl solubility-controlling minerals. The Teloua groundwater is undersaturated with respect to calcite $CaCO_3$ and magnesite $MgCO_3$, which is consistent with the rare occurrence of carbonate minerals found in the rock. Also, the groundwater is close to equilibrium with chalcedony. These results are in line with the literature, which indicates that in the Sahelian aquifer, recharge water is usually Ca^{2+}, Na^+, and HCO_3^- dominated and becomes Na^+ and HCO_3^- dominated in the confined zone (Andrews et al., 1994). Those waters from the literature are in equilibrium with chalcedony and calcite. Sulfate contents are usually strongly undersaturated with respect to gypsum ($CaSO_4{:}2H_2O$), although barite $BaSO_4$ is generally in equilibrium with the aquifer groundwater.

The sampled water also contains nitrates (NO_3^- anions). In some natural circumstances, water which infiltrated during the warming period can show NO_3^- concentrations as high as 80 mg/L by paleo-recharge during the Holocene (Dodo and Zuppi, 1999). Such high NO_3^- concentrations could be due to major paleo-meteorological events that stored organic matter from the surface vegetation and soil by infiltration. Nitrate contamination can also be correlated to human activities. Huneau et al. (2011) studied the groundwater quality within the Sahelian region of the Taoudeni sedimentary basin (Burkina Faso, Mali). They observed that its tendency towards Cl–NO_3–SO_4–HCO_3 water types indicates the anthropogenic influence on groundwater related to the poor sanitary conditions observed around wells. Such an anthropogenic contaminated input, such as fertilizers and/or wastewater, was also found in groundwater resources of the Taoudeni aquifer system in the Sahel region (Trabelsi et al., 2024).

The natural uranium concentration is low, around 15 to 20 μg/L (about 10^{-7} mol/L), and below the recommendation of the world health organization of 30 μg/L (World Health Organization, 2022). U(VI)-minerals in

Table 5
Saturation indices (SI) calculated for the initial hydrochemistry of the Teloua aquifer groundwater and the contaminant aqueous source terms (temp = 30 °C).

Mineral	Teloua aquifer	Moderate source term	High source term
Calcite	−1.1	0.1	0.9
Dolomite	−1.7	0.4	1.9
Gypsum	−4.1	−1.4	−0.2
Chalcedony	0.3	0.3	0.5
Quartz	0.8	0.8	0.9
$UO_3{:}2H_2O$ (schoepite)	−3.3	−3.7	−3.8
$(UO_2)_2SiO_4{:}2H_2O$ (soddyite)	−6.2	−5.6	−7.0
$NaUO_2SiO_3OH{:}H_2O$ (Na-Boltwoodite)	−3.3	−2.0	−2.3
$Ca(UO_2)_2(SiO_3OH)_2{:}5H_2O$ (uranophane)	−3.9	−2.8	−3.3
$Ca(UO_2)_2(PO_4)_2{:}6H_2O$ (autunite)	−1.5	−2.1	−2.9

Table 4
Chemistry of the Teloua aquifer (natural groundwater) and the contaminant source terms (ST) in mg/L.

Total concentration [mg/L]	Teloua aquifer		Moderate source term		High source term		WHO potability guideline
	Sample	Model	Sample	Model	Sample	Model	
pH	7.5	7.5	7.4	7.4	7.4	6.6	6.5–9.5
Na^+	11	11	174	174	486	486	200
K^+	2.5	2.5	2	2	7	7	–
Mg^{2+}	5	5	30	30	200	200	50
Ca^{2+}	8	8	77	70	544	528	–
H_4SiO_4	64	31	67	31	98	31	–
HCO_3^-	76	68	267	256	537	605	–
F^-	0.15	–	0.06	–	< 0.05	–	1.5
Cl^-	1.5	1.5	82	82	110	110	250
NO_3^-	12	12	84	84	430	430	50
PO_4^{3-}	0.7	–	0.1	–	0.25	–	–
SO_4^{2-}	2	2	330	330	2300	2300	250
Charge balance	−3.5 %	–	−4 %	–	−1 %	–	–
Al	< 0.010	–	0.01	–	< 0.010	–	0.1
As	< 0.002	–	< 0.002	–	< 0.002	–	0.01
Ba	0.104	–	0.075	–	0.137	–	1.3
Co	< 0.005	–	< 0.005	–	< 0.005	–	–
Cu	< 0.010	–	< 0.010	–	< 0.010	–	2
Fe	0.066	–	0.101	–	0.083	–	0.2
Mn	< 0.010	–	< 0.010	–	0.002	–	0.08
Mo	< 0.005	–	< 0.005	–	0.01	–	0.07
Ni	< 0.005	–	< 0.005	–	0.009	–	0.07
Pb	< 0.002	–	< 0.002	–	< 0.002	–	0.01
Se	< 0.002	–	< 0.002	–	0.01	–	0.04
U	0.013	0.013	7	7	55	55	0.03
V	< 0.005	–	0.013	–	0.006	–	–
Zn	< 0.010	–	0.012	–	0.014	–	3

an oxidizing geological environment generally consist of schoepite (UO_3:$2H_2O$), silicates (e.g. soddyite ($(UO_2)_2SiO_4$:$2H_2O$), Na-boltwoodite $NaUO_2SiO_3OH$:H_2O, uranophane $Ca(UO_2)_2(SiO_3OH)_2$:$5H_2O$), and phosphate (e.g. autunite $Ca(UO_2)_2(PO_4)_2$:$6H_2O$) (Finch and Murakami, 1999; Smedley and Kinniburgh, 2023). The natural groundwater is strongly under-saturated with respect to all these minerals. In particular, the natural concentration of dissolved phosphates is not high enough to form uranyl-phosphate minerals.

Besides uranium, the concentrations of all the measured trace elements in Teloua groundwater (including possibly toxic elements such as arsenic, copper, lead, and zinc) are very low and significantly below the WHO potability guidelines (2022).

3.1.4. Modeled groundwater chemistry, sorption and reactive mineralogy

To simplify the calculations, only the major elements and uranium were included in the model. Most of the pH and total concentrations of the groundwater in the model were set equal to the measured ones. In the model, the silica concentration of the groundwater was equilibrated with chalcedony and the total inorganic carbon (TIC, expressed as total HCO_3 here) by calcite. A small fraction of the CO_2(g) degassed while being pumped from the borehole to the surface and the measurement. It led to some increase of pH and loss of TIC, which could be corrected by fixing equilibrium with calcite in the model of the contaminated waters. The correction remained small, about 10 %. In line with the measured data, fully-oxidizing conditions were assumed, with uranium permanently in the U(VI) redox state. As discussed below, the chemical changes in the natural waters were driven by variations in Ca^{2+}, Mg^{2+}, HCO_3^-, SO_4^{2-} and UO_2^{2+} total concentrations. Therefore, the following secondary minerals that could precipitate, and possibly redissolve, at thermodynamic equilibrium were also added to the model: calcite, gypsum, soddyite, and uranophane.

Clay minerals (tosudite-smectite) and iron oxides (hematite) can affect uranium mobility through sorption reactions. Hematite can sorb UO_2^{2+} (Hsi and Langmuir, 1985), but it was not considered in the model, as it was only identified in the form of a few scattered grains. Due to the lack of specific data in the literature, tosudite was assimilated to pure montmorillonite whose content was adapted to reproduce the cation exchange capacity (CEC) measured on the total rock. The CEC was set to 3 meq/100 g of rock.

The clay fraction was active as a cation exchanger and for uranium sorption, but it could not dissolve or precipitate. In the absence of laboratory data, the cation equivalent fractions of the model (Table 6) were fixed by imposing equilibrium with the natural groundwater chemistry (Table 4). The divalent cations Ca^{2+} and Mg^{2+} dominate this cationic population. The determination of sorbed uranium was carried out in a similar way, imposing equilibrium with the aqueous concentration of 13 μg/L with the clay exchanger. The resulting solid mass content of uranium (0.9 ppm) is slightly lower than the measured content (1.3 ppm). No uranium minerals were identified by analysis of the cored samples, but it is likely that the sorbed portion represents only a fraction of this total solid uranium. The exchangeable content of 0.9 ppm is, therefore, probably slightly overestimated.

Table 6
Calculated sorbed concentrations of the aquifer bedrock in its natural state included in the model.

Total concentration	Content [meq/100 g of rock]
Cation exchange	
Na^+	0.06
K^+	0.03
Mg^{2+}	1.41
Ca^{2+}	1.50
UO_2^{2+} (1)	~ 0
Cation Exchange Capacity	3
Surface complexation	
Total sorbed UO_2^{2+} (2)	4.3×10^{-4}
Total weak sites ≡ S^wOH	0.138
Total strong site ≡ S^sOH	0.007

(1) Only as uranyl cations, (2) cumulative sorption of uranyl, uranyl hydroxide and uranyl carbonate surface complexes (Table 2).

3.2. Contaminant source term chemistry

3.2.1. Past contaminant leakages

In the COMINAK mine facilities, the treatment of the uranium ores was performed with sulfuric acid and a little nitric acid. This leaching process oxidizes tetravalent uranium U(IV) from the ore to give solubilized hexavalent U(VI). While the COMINAK mine was still in production, aqueous leakage events had increased the aqueous concentrations of U(VI) and SO_4^{2-} very locally in the water beneath the waste facility. A piezometric dome was generated by those localized seepages. The contamination migrated towards a local conductive fault (Fig. 1) but stayed within the perimeter of the mining site by means of a hydraulic containment system consisting of several wells. Monitoring of the mining waters' chemistry is conducted for the purpose of evaluating the effectiveness of the water remediation.

3.2.2. Chemistry of the contaminant source terms

Table 4 indicates that uranium, nitrate and sulfate are the main contaminants. Comparison with the Teloua geochemical background reveals an increase in sulfate and uranium aqueous concentrations by a factor of approximately 1000. These shallow waters were not at acidic pH. The acidity was probably neutralized by the environment at the location of the permeable fault. Tosudite, smectite and carbonate minerals (calcite and dolomite) can neutralize an acid plume through ion exchange and dissolution reactions. The dissolution of calcite and dolomite ($MgCa(CO_3)_2$) leads to an additional enrichment in Ca^{2+}, Mg^{2+}, and HCO_3^- of the affected porewater. The calculation of saturation indices (Table 5) indicates that the high contaminant source term (ST) was supersaturated with respect to calcite and close to equilibrium with gypsum. As mentioned, this calcite 'supersaturation' was probably due to CO_2 degassing during sampling. The modeled data of Table 4 were thus corrected for this sampling artifact and equilibrated with chalcedony and calcite.

Table 4 gives the aqueous chemistry of the impacted waters. The degree of impact differs between the two sampled boreholes. The so-called "moderate-contaminant source term (moderate-ST)" has total concentrations of uranium and sulfate of 7 and 330 mg/L, respectively. The so-called "high-contaminant source term (high-ST)" presents total concentrations of uranium and sulfate of 55 and 2300 mg/L, respectively; that is to say it is about 7 times more concentrated than for the moderate ST. The ratio between the total concentrations of nitrate is about 5. Therefore, the moderate ST could be the result of the dilution of the high ST by the Teloua groundwater.

These two types of impacted waters were used as reference source terms in the presented model, for the purposes of comparison.

4. U(VI) speciation and sorption in the Teloua aquifer

4.1. Occurrence of $(Ca/Mg)_nUO_2(CO_3)_3^{(4-2n)-}$ complexes

As indicated by the calculated saturation indices of Table 5, the contaminated water is undersaturated with respect to all U(VI) minerals. The apparent solubility was likely increased by the formation of strong $Ca_nUO_2(CO_3)_3^{(4-2n)-}$ and $Mg_nUO_2(CO_3)_3^{(4-2n)-}$ complexes that could form under the physicochemical conditions in the impacted waters (Stewart et al., 2010; Shang et al., 2023). Such ternary complexes were clearly identified in the TRLFS scans of the two samples representative of the contaminant source term. The hypsochromic shift relative to the known bands from UO_2^{2+} (Bell and Biggers, 1965) has been first evidenced by Bernhard et al. (1996) and recently modeled using ab initio calculations by Oher et al. (2020). However, the sample from the pristine Teloua aquifer did not contain enough uranium to give a satisfactory spectrum.

The luminescence spectra of uranium were compared to a known synthetic solution from Shang et al. (2023). Normalizing each spectrum to the same area enables direct comparison (Fig. 2). It seems clear that the spectra of the two samples are identical and show fluorescence band positions characteristic of $Ca_nUO_2(CO_3)_3^{(4-2n)-}$ complexes observed both in laboratory thermodynamic studies (Shang and Reiller, 2020, and references therein) and also in field water samples (Tullborg et al., 2017; Shang et al., 2023).

Fig. 3 shows the relative proportions of the main U(VI) aqueous complexes calculated by the model. The speciation of the contaminated STs agrees with the TRLFS analysis. The two predominant species are $CaUO_2(CO_3)_3^{2-}$ and $Ca_2UO_2(CO_3)_3$, the latter being in a higher proportion in the most contaminated water, in agreement with the variation of Ca^{2+}, HCO_3^-, and H^+ activity products (Shang et al., 2023). $MgUO_2(CO_3)_3^{2-}$ is the third most abundant species, in agreement with lower concentration, or lower activity ratios, of Mg^{2+} compared to Ca^{2+} (Shang et al., 2023). These three complexes account for more than 98 mol% of the total inventory of dissolved uranium for the contaminated porewaters. These complexes also represent the main fraction in the natural groundwater of the Teloua aquifer. It must be recalled that the differences in the TRLFS spectra of the $M_nUO_2(CO_3)_3^{(4-2n)-}$ species at difficult to evidence using a 300 lines/mm grating at ambient temperature (Oher et al., 2020; Shang and Reiller, 2021). A more dispersive grating (Oher et al., 2020; Shang and Reiller, 2021) or the use of cryogenic set-up (Wang et al., 2004) would help differentiate these species. The different binary $UO_2(CO_3)_n^{2-2n}$ complexes are also present at the maximum proportion of 15 mol% in the aquifer and decreasing in the contaminated porewaters; the most abundant being $UO_2(CO_3)_2^{2-}$.

4.2. Effect of water chemistry on U(VI) sorption

U(VI) sorption is strongly dependent on the level of modification of the porewater chemistry. In pure water, U(VI) is in the form of the cationic molecule UO_2^{2+} in solution. Regarding the surface acidity properties, the higher the pH, the less positive and more negative the clay, and the higher the sorption of U(VI). Sorption can decrease to some extent at pH > 9. However, at pH in the range 6–9, U(VI) sorption can be considerable with distribution coefficients Kd of the order of 10,000 to

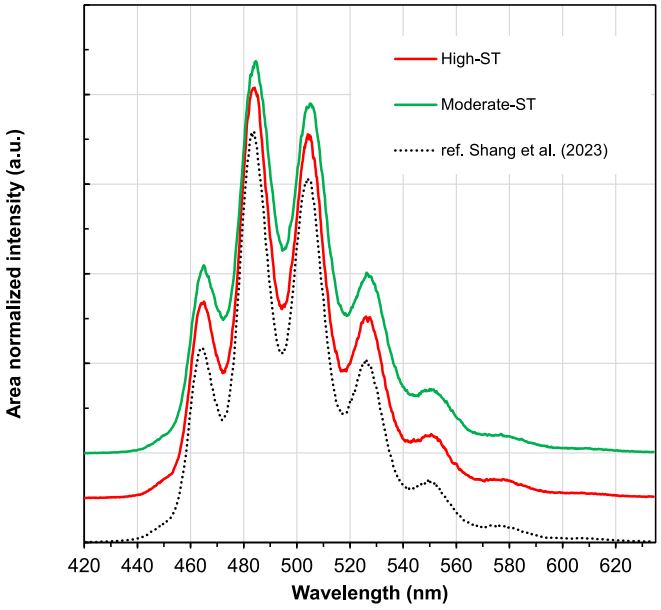

Fig. 2. Fluorescence spectra of the contaminant high and moderate source-terms normalized to the same area, and offset vertically for readability, compared with the reference spectrum for a solution containing $Ca_nUO_2(CO_3)_3^{(4-2n)-}$ complexes by Shang et al. (2023).

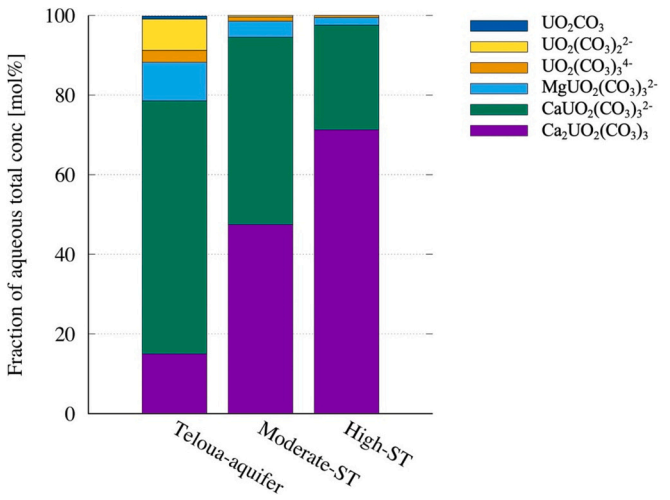

Fig. 3. Calculated speciation of the main U(VI) complexes showing a progressive change from natural background conditions to the contaminated porewaters.

100,000 L/kg on Na-montmorillonite (Marques Fernandes et al., 2012; Baeyens et al., 2014; Tournassat et al., 2018). But in more complex aqueous solutions, the amount of sorbed U on clay and related Kd values could drop by two or three orders of magnitude in contaminated water conditions, due to the formation of clearly-identified (Ca, $Mg)_nUO_2(CO_3)_3^{(4-2n)-}$ complexes (Tournassat et al., 2018; Montavon et al., 2022; Stockmann et al., 2022). For these reasons, all aspects of water chemistry must be taken into account (pH, dissolved calcium and bicarbonate contents in particular) to properly simulate the behavior of uranium in the Teloua aquifer impacted by mining activities.

Fig. 4 shows the results of the batch geochemical modeling of the porewater chemistry changes during the propagation of the contaminated water into the Teloua aquifer. More precisely, the model focuses on one element of volume (i.e. one node of a grid) of the aquifer containing 8 vol% of water and 92 vol% of the minerals (including the sorbing clay-phase). The aqueous phase volume V_0 was then progressively replaced five times ($V/V_0 = 5$) by an equivalent volume of the contaminated water. This modeling was chosen to mimic the effect of the progression of the plume within the aquifer while emphasizing the chemical processes. This progression (x axis) is represented in a log scale in Fig. 4 due to the relatively fast changes of the chemistry during the propagation. The factor $V/V_0 = 5$ is sufficient for the changes of the chemistry of the water from pristine to contaminated to be in agreement with the data of Table 4, as shown for the pH in Fig. 4a and the concentrations of Ca^{2+} and HCO_3^- in Fig. 4b. The two types of contaminant ST (moderate and high) are shown. Those changes are generally smooth during the progression, except at $V/V_0 = 0.2$ for the high ST and $V/V_0 = 1$ for the moderate ST, due to calcite precipitation (in a small amount, Fig. SI-1a).

The contamination of the groundwater by NO_3^- and SO_4^{2-} (Fig. 4c) is perfectly continuous, with a progressive replacement of the natural water by the contaminated ones. In particular, water saturation with respect to gypsum is never reached, which otherwise could have controlled SO_4^{2-} solubility (no concentration plateau). The change in U (VI) aqueous concentration (Fig. 4d) is driven by three interdependent processes. Firstly, as for NO_3^- and SO_4^{2-}, the physical replacement of the pristine Teloua water by the contaminated. Secondly, and differently from those anions, U(VI) is partly removed from the solution by sorption onto the clay exchanger present in the Teloua rock. However, thirdly, sorption is weak, due to the formation of aqueous complexes that retain U(VI) in solution and prevent sorption. These complexes are affected by the break in the (bi)carbonate concentration (Fig. 4b) due to calcite precipitation. That is to say that the limit in carbonate maximal

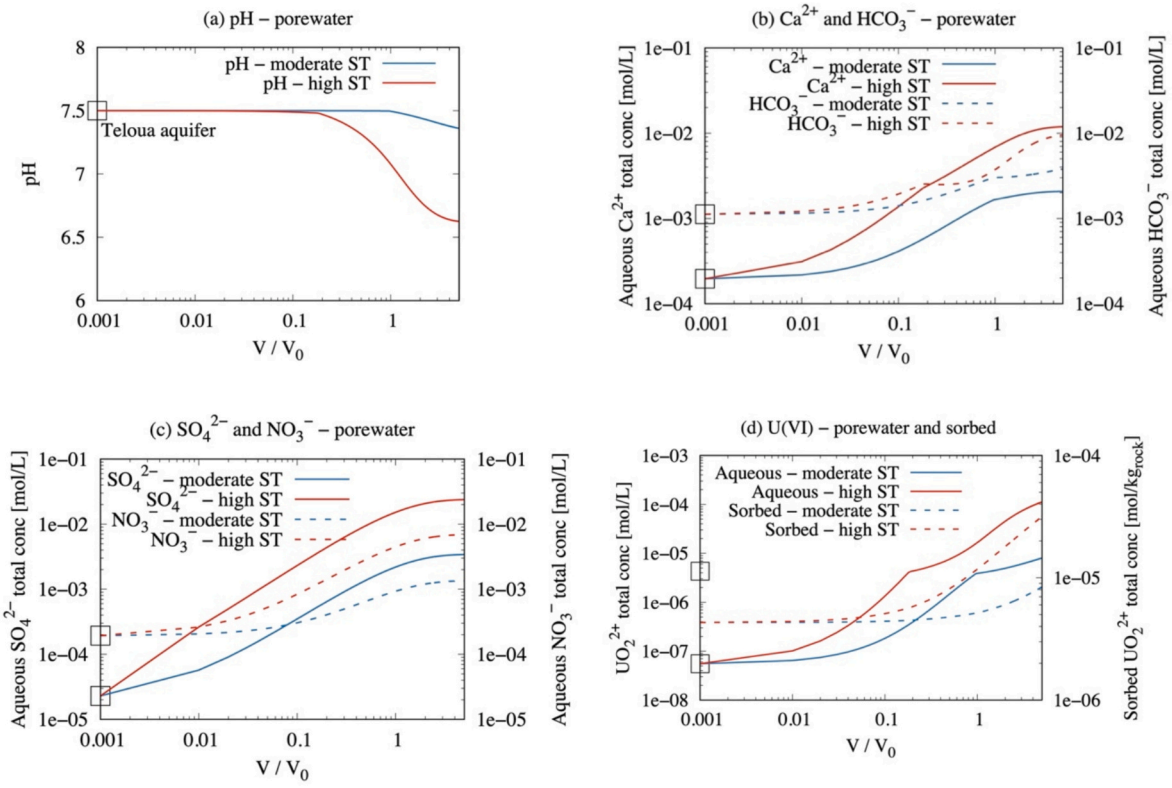

Fig. 4. Batch modeling of changes to porewater chemistry of the Teloua aquifer when the pristine water volume V_0 is progressively replaced five times by an equivalent volume of the contaminated water., for the two types of source term (ST); the empty square symbols represent the pristine Teloua aquifer.

concentration (and to a lesser extent Ca^{2+} maximal concentration), probably due to the precipitation of calcite, constrains the maximal concentration of the ternary complexes.

When comparing the dissolved and sorbed concentrations, it can be seen that sorption is very effective in the natural Teloua groundwater but virtually non-existent at high ST, as the sorbed concentration is lower than the aqueous concentration. In Fig. 4d, the sorbed concentration is expressed in the same units as the aqueous for the purposes of comparison. Fig. SI-1b shows the U(VI) sorbed concentration in mol/kg of rock. The results of the same geochemical modeling were then used to calculate the corresponding Kd values of U(VI) according to Eq. 2. The Kd value progressively decreases by three orders of magnitude (Fig. 5a). For the pristine Teloua aquifer it is about 75 L/kg, decreasing to 1 L/kg at moderate ST, and down to 0.03 L/kg at high ST. As explained above, this decrease is mainly due to the uranium desorption by a thermodynamic equilibrium shifted in favor of the ternary $Ca_nUO_2(CO_3)_3^{(4-2n)-}$ complexes in solution, which become increasingly stable as $Ca^{2+}(Mg^{2+})$–HCO_3^- is added to the geochemical system.

In order to give a more detailed interpretation of the modeling results, Fig. 5b shows the changes during the plume propagation of the concentrations of the U(VI) species that can participate in the sorption mechanisms in the present model (Table 2). Firstly, it is worth noting that the model also indicates that the complexes $UO_2(CO_3)_2^{2-}$ and $UO_2(CO_3)_3^{4-}$ make a significant contribution, although lower than the ternary ones, to the aqueous complexation. The latter species is not shown in Fig. 5b because it cannot sorb, according to Marques Fernandes et al. (2012). This is probably due to its high negative charge, which is also responsible for the relatively low contribution of the former species to sorption, of around 10 mol% (Fig. 5c). According to the model, the major sorbed species is the neutral $UO_2(CO_3)$ (90 mol%), for both the pristine Teloua groundwater and the contaminated porewater. The dashed line in Fig. 5a (denoted as "low sorption") is an alternative way of demonstrating the importance of the sorption of $UO_2(CO_3)_n^{(2-2n)}$ complexes. It has been calculated only with the sorption of UO_2^{2+} and $UO_2^{2+} - OH^-$ complexes. The corresponding Kd values are clearly lower than those calculated with the full sorption set, showing again the importance of the uranyl-carbonate complexes in this model. It is worth noting that the model's definition of the initial state of the pristine Teloua aquifer is also unsatisfactory when the sorption of uranyl-carbonate is removed.

5. Migration of sulfate and U(VI) within the Teloua aquifer

5.1. Simplified migration parameters

The changes in porewater chemistry and the contaminant plume migration have been estimated by a simplified reactive transport model based on a 1D flow line (Fig. 1). This model has been created to support the various rehabilitation scenarios. It takes into account the specific physicochemical conditions of the groundwater of arid and semi-arid sub-Saharan regions and the mineral retention properties of the geological formation. In the present case, the natural attenuation distances for dissolved uranium migration are evaluated as if no remediation action is taken, as part of a conservative approach.

Calibrated on field data, the mean hydraulic conductivity was set to 3×10^{-5} m/s with an effective porosity of 0.08 and longitudinal dispersivity of 50 m. The effective Darcy flow was fixed at 0.25 m/year assuming fully water-saturated conditions. This flow is low but still above typical recharges from the region (Dodo and Zuppi, 1999). For instance, the mean recharge rate is in the order of 5 mm/y in an unconfined aquifer of the semi-arid area of the Iullemeden Basin in Niger (La Salle et al., 2001).

5.2. Sulfate as a tracer of the furthest extent of the plume

Fig. 6a shows the progressive advective migration of SO_4^{2-} within the

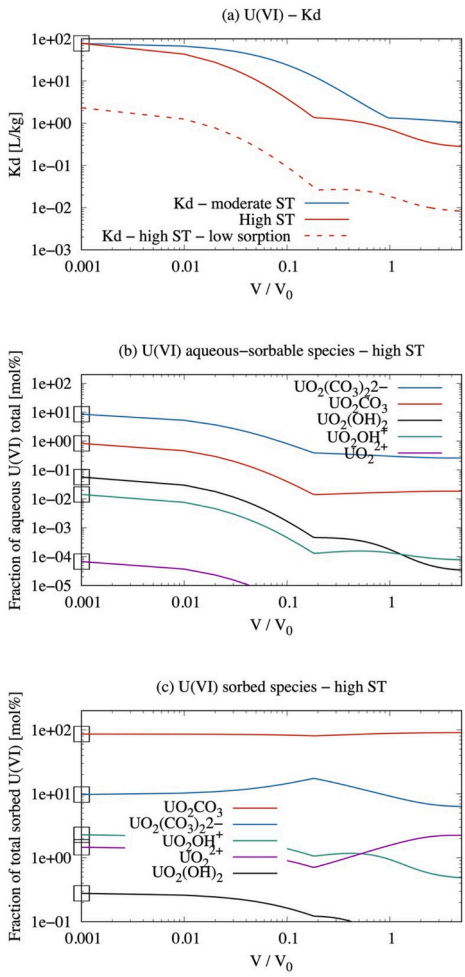

Fig. 5. Batch modeling of (a) the change of Kd of U(VI) and (b,c) of the U(VI) species participating in sorption on the Teloua bedrock, when the pristine water volume V_0 is progressively replaced five times by an equivalent volume of the contaminated water, for the two types of source term (ST); the empty square symbols represent the pristine Teloua aquifer.

Teloua aquifer. The progressive slope of the concentration profile is due to hydrodynamic dispersion. The front is estimated to move approximately 300 m after 100 years, 1.5 km after 500 years and up to 3 km after 1000 years.

The increase of SO_4^{2-} concentration during the propagation of the contamination plume can be regarded as a tracer of the furthest extent of the plume, for four reasons. Firstly, SO_4^{2-} concentration is about 1000 times higher in the plume than in the pristine groundwater. Secondly, bacterial sulfate reduction is impossible due to the lack of dissolved organic matter and the oxidizing conditions prevailing in the Teloua aquifer. Thirdly, while sulfate could be attenuated by gypsum precipitation, the saturation indices in Table 5 suggest that the contaminated waters downstream from the fault are very close to being at equilibrium with gypsum. However, the Teloua natural groundwater is highly undersaturated with respect to gypsum due to the low concentrations of both Ca^{2+} and SO_4^{2-}. Therefore, the mixing of the contaminated water and the pristine is not likely to lead to any gypsum formation. This is confirmed by the presented 1D reactive transport model. Lastly, sulfate sorption on the clay fraction in the Teloua bedrock can be considered as negligible. SO_4^{2-} is a negatively double-charged ion that sorbs onto positively charged mineral surfaces at acidic to very acidic pH values, but not at neutral pH (Zachara et al., 1988; Bazer-Bachi et al., 2007). Thus, SO_4^{2-} can be considered as a tracer.

5.3. Migration of mining U(VI) and desorption of natural U(VI)

As a prerequisite to the analysis of U(VI) migration, Fig. 6b and Fig. SI-2 show the spatial extent of the effects on the porewater chemistry caused by the contaminated source terms. The chemistry will be greatly altered over about 1.5 km after 500 years. The profiles of the Ca^{2+} and HCO_3^- concentrations are more complex than in the batch modeling shown in Fig. 4 but, overall, there is strong agreement between the batch and reactive transport models. The Ca^{2+} concentration is increased by two orders of magnitude, the HCO_3^- concentration by one. The latter is again limited by the precipitation of calcite (Fig. SI-3). The cation concentrations in the porewater are also affected by cationic exchanges (Fig. SI-4). This process and also calcite precipitation cause the small fluctuations in the Ca^{2+} profiles in Fig. 6b.

Fig. 6c shows the intensity and spatial extent of the U(VI) plume after 500 y. A detailed analysis of the propagation of the uranium plume reveals a dual process of increasing uranium content in porewater. There is, firstly, the migration of uranium from the contaminated water itself, the extent of which is more or less identical to the profiles of high sorbed U(VI) content (Fig. 6d). It is worth mentioning that the absolute amount of sorbed U(VI) is much higher in the reactive transport model than in the batch model since the former corresponds to many more replacements of the pore volume than the latter. Fig. 6d also indicates that the uranium plume of strictly anthropogenic origin is always more spatially restricted (about 500 m after 500 y), even in the case of the highest Ca–HCO_3 content (i.e. the high ST). Nevertheless, there is also a second process contributing to U(VI) concentration increase, this being the desorption of naturally sorbed uranium (Fig. 6d) due to the propagation of the Ca–HCO_3 plume (Fig. 6b), which promotes complexation of uranium in the porewater. The desorption profile follows the HCO_3^- concentration profile with a first wave taking place between 0.5 and 1 km, and a second wave of weaker desorption between 1 and 2 km. The plume propagation of U(VI) from the mine seems realistic, while the process of natural U(VI) desorption due to the farther propagation of the Ca – HCO_3 plume remains a modeling assumption.

Comparison of the dissolved (Fig. 6c) and sorbed (Fig. 6d) U(VI) concentrations indicates that the sorption of mining U(VI) is minimal and aqueous complexation maximal for the high-ST condition. The sorbed to aqueous U(VI) ratio close to the mine is about 1 and 25 for moderate high ST, respectively. It is worth noting that, in both cases, sorption is relatively low. The same ratio is about 2500 in the natural groundwater. The Kd profile calculated along the 1D flowline after 500 y (Fig. SI-5) gives the same information. Kd values close to the mine are 1 and 0.3 L/kg for moderate high ST, respectively. The Kd value for natural groundwater is about 70–80 L/kg.

The possible U(VI) secondary silicate minerals soddyite and uranophane (formulae in Table 5) never precipitated during the modeling: the SI of soddyite ranged from −6 (natural state) to −8 (high ST), and the SI of uranophane from −4 (natural state) to −6 (high ST). The undersaturation was due either to the low U(VI) groundwater content in the natural state or the strong aqueous complexation in the porewater, which increases the apparent solubility of those minerals.

5.4. Natural attenuation of the U(VI) plume after contaminant depletion

The previous calculations were based on a constant source-term injection if no remediation solution was applied. This assumption is highly questionable over 1000 years. A first step to a less pessimistic conservative scenario was, consequently, evaluated by a scenario stating that the contaminated plume was injected during a fixed duration (25 or 250 years) and then replaced by the constant ingress of the natural Teloua groundwater afterwards. Fig. 7a gives a picture of the U(VI) porewater concentration within the flowline after 500 years, with a contamination period of 250 years. This long duration of 250 years is also clearly pessimistic, but it is useful to emphasize the main mechanisms of return to the natural background state.

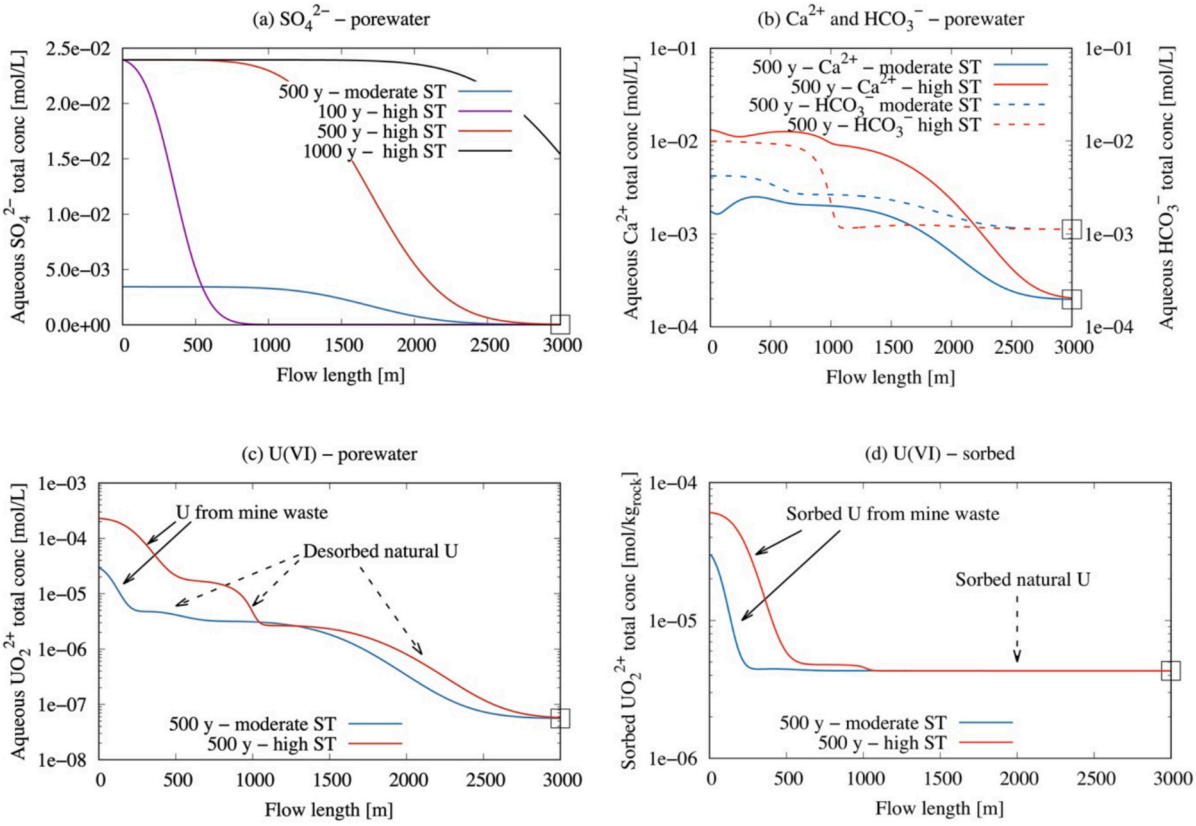

Fig. 6. Reactive transport modeling of the migration of the source terms (ST) within the Teloua aquifer over 1000 years if no remediation solution is applied; the empty square symbols represent the pristine Teloua aquifer.

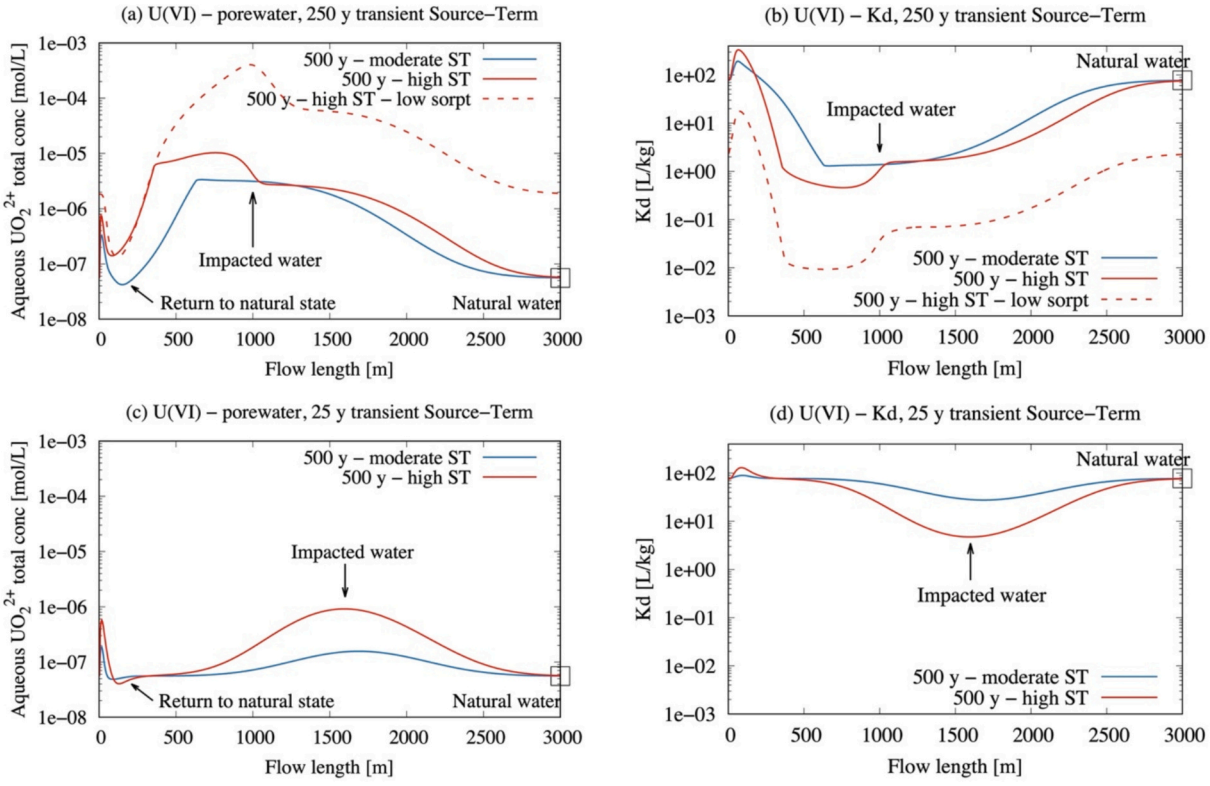

Fig. 7. Reactive transport modeling of the migration distance of the source terms (ST) after 500 years, assuming their depletion after 250 years (a,b) or 25 years (c, d), if no remediation solution is applied.

The ingress of the more diluted groundwater after 250 years induces the gradual return to the natural background U(VI) concentration close to the mine after 500 years. U(VI) concentration very close to the mine is higher than at 100 m due to a higher accumulation of sorbed U(VI) in the former region as shown by Fig. 6d. Fig. 7a also shows that the increase of U(VI) concentration (and the overall chemical changes) in porewater brought by the medium ST requires less time to return to the natural state than the high ST. Nevertheless, in both cases, the accumulation of anthropogenic U(VI) by sorption will constitute a second source term of U(VI) towards porewater, but of much smaller intensity than the primary contamination. Indeed, the condition for high sorption by the ternary complexes will have disappeared by then. The U(VI) aqueous concentration could remain slightly above the natural background state in those zones located close to the former mining site.

Like the batch plume model, the U(VI) migration plume is much more pronounced, in terms of maximal concentration and contamination depth (dashed line in Fig. 7a), while the sorption of $UO_2(CO_3)_n^{(2-2n)}$ complexes onto the clay phases is not included in the model. As for the batch model, the initial state of the pristine aquifer does not seem to be properly modeled with this reduced set of sorption parameters.

Fig. 7b provides the Kd values calculated along the flowline while taking into account the contamination period of 250 years. The same conclusions as for U(VI) concentration can be drawn. In the same range of values obtained with the batch model (Fig. 5a), the natural Kd of about 80 L/kg drops as low as 1 and 0.4 L/kg at the minimum for moderate and high ST, respectively. These altered Kd values rebound when the aquifer is flushed with the pristine groundwater. The Kd values seem to be even higher by a factor of three than in the initial state, apparently because the accumulated anthropogenic (mining) U(VI) on the clay phases will desorb gradually.

The scenario which projects a contamination period of only 25 years (Fig. 7c and d) would give a more representative remediation timescale than that for 250 years. This case does not lead to any significant contamination of the natural groundwater. The U(VI) porewater concentration increases by a factor 20 at worst, and then returns to the natural chemical background of the Teloua aquifer in less than 80 years.

5.5. Comparison with the literature

5.5.1. Sorption onto $UO_2(CO_3)_n^{(2-2n)}$ complexes

In addition to the study by Marques Fernandes et al. (2012) used in the present modeling, Montavon et al. (2022) also showed that the sorption of uranyl-carbonate surface complexes had to be included to obtain a satisfactory level of agreement between the model and the experiment on U(VI) retention by the Callovo-Oxfordian claystone. Mei et al. (2022) modeled U(VI) sorption on illite using a two-site non-electrostatic surface complexation and cation exchange model. Two ternary surface complexation reactions with carbonate were needed to describe the experimental sorption data, in addition to binary and ternary hydroxo-uranyl surface complexation reactions. In contrast, the model of Stockmann et al. (2022) did not require any ternary uranyl carbonate surface complexes to correctly describe their batch experiments of U(VI) sorption onto montmorillonite in contact with a $CaCl_2$ solution at neutral pH and in the presence of CO_2. Similarly, Tournassat et al. (2018) stated that U(VI) sorption onto montmorillonite under real atmospheric conditions could be modeled without the formation of uranyl carbonate surface complexes.

Besides clay phases, the modeling of experiments of U(VI) sorption by surface complexation onto ferrihydrite in competition with the aqueous ternary $Ca_nUO_2(CO_3)_3^{(4-2n)-}$ complexes also took into account the ternary surface complexation of the $UO_2(CO_3)_n^{(2-2n)}$ species (Fox et al., 2006). Stewart et al. (2010) demonstrated that ternary $Ca_nUO_2(CO_3)_3^{(4-2n)-}$ complexes were unreactive with the mineral surface but free ion, hydroxo-uranyl, and carbonato-uranyl surface species were required to correctly describe uranium adsorption on to synthetic and natural sediments. Wang et al. (2013) investigated U(VI) sorption on manganese oxides by X-ray absorption spectroscopy and surface complexation modeling. Their surface complexation model included inner-sphere monodentate and bidentate surface complexes and one uranyl-carbonate surface complex, which was consistent with their EXAFS analysis.

To conclude, the reality and importance of sorption by surface complexation of uranyl-carbonate species onto different types of minerals is still a matter of debate in the scientific community. The present modeling study was mainly based on $UO_2(CO_3)_n^{(2-2n)}$ sorption, especially the neutral $UO_2(CO_3)$ complex, onto a tosudite surface. As a matter of fact, although not yet proven, the initial state seems to be better modeled under this assumption. The sensitivity analysis indicated that U(VI) sorbed concentration and the calculated Kd values would be at least 10 times lower if these surface complexes were not included in the model.

5.5.2. U(VI) Kd values of natural rocks containing clay phases

With respect to clayey rocks, Baeyens et al. (2014) studied sorption onto Opalinus clay containing 40 wt% of clay phases (illite and interstratified illite/smectite) and a solution of pH 8.0, Ca^{2+} and HCO_3^- total concentration of 3×10^{-2} M and 2×10^{-4} M, respectively. The mean measured Kd value was found to be around 100 L/kg for U(VI) concentrations below 0.5 mg/L (this Kd would become 15 L/kg if it was normalized to the 5 wt% clay-content of the Teloua sandstone). Tournassat et al. (2018) made U(VI) sorption experiments on pure Na-montmorillonite at Ca^{2+} and HCO_3^- total concentration of 2×10^{-3} M and 5×10^{-4} M, respectively. The measured Kd values were about 1000 L/kg at pH 7.5 and 100 L/kg at pH 8.5 (corresponding to 50 and 5 L/kg, respectively, when normalized to the Teloua clay content). Montavon et al. (2022) reported that the retention of U(VI) on the Callovo-Oxfordian (COx) claystone was lower (Kd $\leq$ 5 L/kg) due to the formation of soluble ternary $Ca_nUO_2(CO_3)_3^{(4-2n)-}$ complexes in the synthetic COx porewater.

With respect to carbonate rocks, Baeyens et al. (2014) studied the sorption of uranyl ions on Effingen limestone in lab tests. The bedrock contained 7 wt% of clay phases (illite and interstratified illite/smectite) in contact with a solution of pH 8.0, Ca and HCO_3^- total concentration of 6×10^{-2} M and 10^{-4} M, respectively. The proportion of clay is similar to the Teloua bedrock and the water chemistry is intermediate between the natural Teloua water and the moderately contaminated water (moderate ST). The mean measured Kd value was found to be around 10 L/kg for U(VI) concentration below 5 mg/L, and 4 L/kg at a U concentration of 25 mg/L.

With respect to sandstone, (Yang et al., 2023) studied the U(VI) sorption capacity of sandstone samples from an aquifer located downstream from a mining area in China. A higher content of clay was associated with a higher U-adsorption capacity of the sandstones. Under the same experimental conditions (Na_2SO_4 solution in contact with atmospheric CO_2, pH 8), U(VI) Kd was 50 % lower for the column experiments (0.07 L/g, i.e. 70 L/kg) than that obtained from the batch sorption experiments (0.14 L/g, i.e. 140 L/kg).

The calculated U(VI) Kd of the pristine Teloua aquifer of 80 L/kg is within the right order of magnitude of these published Kd values (from 10 to 50 L/kg when the clay content is normalized to the Teloua one, except that those of Yang et al. (2023) seem to be lower). Both in the literature and the present modeling study, the Kd will significantly drop when the aqueous chemistry becomes more concentrated in Ca-HCO_3 and/or the pH become slightly more alkaline.

6. Conclusion

Sandstone-hosted uranium deposits are mined in the Sahel regions. As in most sub-Saharan aquifers, the local groundwater presents a strong oxidizing signature and very low water recharge. Determining the baseline of any anthropogenic activity for uranium, which is usually considered as immobile in most aquifers worldwide, is a key issue in such aquifers. This study offers new and complementary insights that are

relevant for the still poorly known environmental chemistry of uranium in aquifers from semi-arid and arid regions on Earth. Firstly one provides rare in-situ sampling of both contaminated and pristine groundwater at the COMINAK mine in Niger: the major as well as several trace elements were analyzed. Secondly, based on mineralogical and petrophysical parameters acquired previously from the bedrock, a realistic model has been developed, progressing from a batch geochemical model to a 1D reactive transport model with different contamination scenarios. The variability of sorption efficiency was addressed via a sensitivity analysis to uranyl complex speciation and translated in terms of Kd distribution coefficients.

In both the natural and the locally-impacted zones of the Teloua aquifer, uranium is present in its most oxidized redox state U(VI), as uranyl cations that can be strongly stabilized in solution as $Ca_nUO_2(CO_3)_3^{(4-2n)-}$ complexes. The literature and present modeling also indicate that the sorption of $UO_2(CO_3)_n^{(2-2n)}$ onto clay phases of the natural rock can play a key role in the immobilization of U(VI). In this context, the current study highlights the importance of integrating water chemistry and sorption processes to effectively model the speciation and migration of uranium within the Teloua aquifer, which has been partially impacted by mining activities. In particular, the modeled amount of sorbed U could drop by two or three orders of magnitude in altered water chemistry, due to the formation of $Ca_nUO_2(CO_3)_3^{(4-2n)-}$ complexes that are clearly demonstrated by TRLFS acquisition on the sampled porewater. Confirmation of the sorption properties of the Teloua bedrock as a function of water chemistry could be obtained by dedicated lab batch experiments, despite the inherent challenges and time-consuming nature of such experimental investigations.

The mitigating factor for sulfate is gypsum precipitation close to the source term and then dispersion/dilution within the aquifer, in which SO_4^{2-} anions behaved like a perfect tracer. The propagation of the uranium plume has revealed a dual process combining the propagation of anthropogenic U(VI) from the mine to the process of natural U(VI) desorption due to the propagation of the Ca – HCO_3 plume deeper in the aquifer. The mitigating factors for U(VI) are sorption on the tosudite clay phase as well as the dispersion/dilution of the contaminated source terms in the natural groundwater, in which the strong $Ca_nUO_2(CO_3)_3^{(4-2n)-}$ complexes are less important and, consequently, enable U(VI) sorption. The calculated Kd values vary from 80 L/Kg for the natural state to 1 and 0.3 L/kg for the moderate and high source terms, respectively. Overall, there should be an efficient immobilization of fixed uranium by natural attenuation once the contaminant source term has become depleted.

CRediT authorship contribution statement

L. De Windt: Validation, Methodology, Investigation, Formal analysis, Conceptualization, Writing – review & editing, Writing – original draft. **P. Grizard:** Validation, Resources, Methodology, Formal analysis, Data curation, Conceptualization, Writing – review & editing. **C. Besançon:** Validation, Methodology, Investigation, Formal analysis, Conceptualization. **F. Assalack:** Resources, Data curation. **I. Djibo Hama:** Resources, Data curation. **P.E. Reiller:** Validation, Methodology, Investigation, Writing – review & editing. **N. Seigneur:** Methodology, Formal analysis, Writing – review & editing. **M. Descostes:** Validation, Project administration, Methodology, Conceptualization, Writing – review & editing.

Declaration of competing interest

The authors declare that they have no known competing financial interests or personal relationships that could have appeared to influence the work reported in this paper.

Data availability

Data will be made available on request.

Acknowledgements

The authors thank the reviewers for their relevant comments and suggestions. They also gratefully acknowledge the workers from COMINAK mine for their effort and collaboration for the sampling and the shipment of the samples for dedicated analyses.

Appendix A. Supplementary data

Supplementary data to this article can be found online at https://doi.org/10.1016/j.jconhyd.2025.104507.

References

Abd Elmola, A., Asaad, A., Patrier, P., Beaufort, D., Ballini, M., Descostes, M., 2020. Clay mineral signatures of fault-related fluid flows in a sandstone reservoir: a case study from the Teloua formation, Tim Mersoï Basin, Niger. J. Afr. Earth Sci. 168, 103840.
Andrews, J.N., Fontes, J.C., Aranyossy, J.F., Dodo, A., Edmunds, W.M., Joseph, A., Travi, Y., 1994. The evolution of alkaline groundwaters in the continental intercalaire aquifer of the Irhazer Plain, Niger. Water Resour. Res. 30, 45–61.
Ascani, M., 2021. Cominak - Mine Closure and Remediation, Information Pack Report, Orano (France).
Baeyens, B., Marques Fernandes, M., Bradbury, M.H., 2014. Bentonite with Predictions Using the SGT-E2 Approach to Derive Sorption Data Bases. Technical Report 12-05, Nagra, Wettingen (CH).
Bazer-Bachi, F., Descostes, M., Tevissen, E., Meier, P., Grenut, B., Simonnot, M.O., Sardin, M., 2007. Characterization of sulphate sorption on Callovo-Oxfordian argillites by batch, column and through-diffusion experiments. Phys. Chem. Earth 32, 552–558.
Bell, J.T., Biggers, R.E., 1965. Absorption spectrum of uranyl ion in perchlorate media: part I. Mathematical resolution of overlapping band structure and studies of environmental effects. J. Mol. Spectrosc. 18, 247–275.
Bernhard, G., Geipel, G., Brendler, V., Nitsche, H., 1996. Speciation of uranium in seepage waters of a mine tailing pile studied by time-resolved laser-induced fluorescence spectroscopy (TRLFS). Radiochim. Acta 74, 87–91.
Bradbury, M.H., Baeyens, B., 1997. A mechanistic description of Ni and Zn sorption on Na-montmorillonite part II: modelling. J. Contam. Hydrol. 27 (3–4), 223–248.
Bradbury, M.H., Baeyens, B., 2003. Porewater chemistry in compacted re-saturated MX-80 bentonite. J. Contam. Hydrol. 61, 329–338.
Brown, G., Bourguignon, P., Thorez, J., 1974. A lithium-bearing aluminian regular mixed layer montmorillonite-chlorite from Huy, Belgium. Clay Miner. 10 (3), 135–144.
Burow, K.R., Belitz, K., Dubrovsky, N.M., Jurgens, B.C., 2017. Large decadal-scale changes in uranium and bicarbonate in groundwater of the irrigated western U.S. Sci. Total Environ. 586, 87–95.
de Boissezon, H., Levy, L., Jakymiw, C., Distinguin, M., Guerin, F., Descostes, M., 2020. Modeling uranium and 226Ra mobility during and after an acidic in situ recovery test (Dulaan Uul, Mongolia). J. Contam. Hydrol. 235, 103711.
Dodo, A., Zuppi, G.M., 1999. Quaternary climatic variability in the Tarat aquifer (Arlit, Niger). Compt. Rend. l'Acad. Sci.-Ser. IIA-Earth Planet. Sci. 328, 371–379.
Edmunds, W.M., 2003. Hydrogeochemical processes in arid and semi-arid regions—Focus on North Africa. In: Simmers, I.Ed. (Ed.), Understanding Water in a Dry Environment: Hydrological Processes in Arid and Semi-Arid Zones. CRC Press, pp. 251–287.
Escario, S., Seigneur, N., Collet, A., Regnault, O., de Boissezon, H., Lagneau, V., Descostes, M., 2023. A reactive transport model designed to predict the environmental footprint of an 'in-situ recovery' uranium exploitation. J. Contam. Hydrol. 254 art. no. 104106.
Finch, R., Murakami, T., 1999. Systematics and Paragenesis of Uranium Minerals, in Review in Mineralogy 38 « Uranium: Mineralogy, Geochemistry, and the Environment », 91–180.
Fox, P.M., Davis, J.A., Zachara, J.M., 2006. The effect of calcium on aqueous uranium (VI) speciation and adsorption to ferrihydrite and quartz. Geochim. Cosmochim. Acta 70, 1379–1387.
Garcia-Rios, M., De Windt, L., Luquot, L., Casiot, C., 2021. Modeling of microbial kinetics and mass transfer in bioreactors simulating the natural attenuation of arsenic and iron in acid mine drainage. J. Hazard. Mater. 405, 124133.
Hsi, C.D., Langmuir, D., 1985. Adsorption of uranyl onto ferric oxyhydroxides: Application of the surface complexation site-binding model. Geochimica et Cosmochimica Acta 49, 1931–1941.
Huneau, F., Dakoure, D., Celle-Jeanton, H., Vitvar, T., Ito, M., Traore, S., Compaore, N.F., Jirakova, H., Le Coustumer, P., 2011. Flow pattern and residence time of groundwater within the south-eastern Taoudeni sedimentary basin (Burkina Faso, Mali). J. Hydrol. 409, 423–439.
La Salle, C.L.G., Marlin, C., Leduc, C., Taupin, J.D., Massault, M., Favreau, G., 2001. Renewal rate estimation of groundwater based on radioactive tracers (3H, 14C) in an unconfined aquifer in a semi-arid area, Iullemeden Basin, Niger. J. Hydrol. 254, 145–156.

Lagneau, V., Regnault, O., Descostes, M., 2019. Industrial deployment of reactive transport simulation: an application to uranium in situ recovery. Rev. Mineral. Geochem. 85, 499–528.
Mamadou, M.M., Cathelineau, M., Deloule, E., Reisberg, L., Cardon, O., Vallance, J., Brouand, M., 2022. The Tim Mersoï Basin uranium deposits (northern Niger): geochronology and genetic model. Ore Geol. Rev. 145, 104905.
Marques Fernandes, M., Baeyens, B., Dähn, R., Scheinost, A.C., Bradbury, M.H., 2012. U (VI) sorption on montmorillonite in the absence and presence of carbonate: a macroscopic and microscopic study. Geochim. Cosmochim. Acta 93, 262–277.
Mei, H., Aoyagi, N., Saito, T., Kozai, N., Sugiura, Y., Tachi, Y., 2022. Uranium (VI) sorption on illite under varying carbonate concentrations: batch experiments, modeling, and cryogenic time-resolved laser fluorescence spectroscopy study. Appl. Geochem. 136, 105178.
Montavon, G., Ribet, S., Loni, Y.H., Maia, F., Bailly, C., David, K., Lerouge, C., Madé, B., Robinet, J.C., Grambow, B., 2022. Uranium retention in a Callovo-Oxfordian clay rock formation: from laboratory-based models to in natura conditions. Chemosphere 299, 134307.
Oher, H., Vercouter, T., Réal, F., Shang, C., Reiller, P.E., Vallet, V., 2020. Influence of alkaline earth metal ions on structures and luminescent properties of $Na_mM_nUO_2(CO_3)_3^{(4-m-2n)-}$ (M = Mg, Ca; m, n = 0–2): time-resolved fluorescence spectroscopy and ab initio studies. Inorg. Chem. 59, 15036–15049.
Reiller, P.E., 2024. Predominance of the alkaline earth (II) triscarbonatoactinyl (VI) complexes in different geochemical contexts: review of existing data and estimation of potentially unidentified species. Chemosphere 350, 141049.
Reiller, P.E., Descostes, M., 2020. Development and application of the thermodynamic database PRODATA dedicated to the monitoring of mining activities from exploration to remediation. Chemosphere 251, 126301.
Seigneur, N., De Windt, L., Déjeant, A., Lagneau, V., Descostes, M., 2021. Long-term evolution of uranium mobility within sulfated mill tailings in arid regions: a reactive transport study. Minerals 11, 1201.
Shang, C., Reiller, P.E., 2020. Determination of formation constants and specific ion interaction coefficients for $Ca_nUO_2(CO_3)_3^{(4-2n)-}$ complexes in NaCl solution by time-resolved laser-induced luminescence spectroscopy. Dalton Trans. 49 (2), 466.
Shang, C., Reiller, P.E., 2021. The determination of the thermodynamic constant of $MgUO_2(CO_3)_3^{2-}$ complex in $NaClO_4$ and NaCl media using time-resolved luminescence spectroscopy, and applications to different geochemical contexts. Dalton Trans. 50, 4363.
Shang, C., Coreau, N., Macé, N., Descostes, M., Reiller, P.E., 2023. Implications of recently derived thermodynamic data and specific ionic interaction theory parameters for $(Mg/Ca)_nUO_2(CO_3)_3^{(4-2n)-}$ complexes on the predominance of the Mg^{2+}–Ca^{2+}–UO_2^{2+}–OH^-–CO_3^{2-} systems, and application to natural and legacy-mine waters. Sci. Total Environ. 858, 159927.
Smedley, P.L., Kinniburgh, D.G., 2023. Uranium in natural waters and the environment: distribution, speciation and impact. Appl. Geochem. 148, 105534.
Stewart, B.D., Mayes, M.A., Fendorf, S., 2010. Impact of uranyl−calcium−carbonato complexes on uranium (VI) adsorption to synthetic and natural sediments. Environ. Sci. Technol. 44, 928–934.
Stockmann, M., Fritsch, K., Bok, F., Fernandes, M.M., Baeyens, B., Steudtner, R., Müller, K., Nebelung, C., Brendler, V., Stumpf, T., Schmeide, K., 2022. New insights into U(VI) sorption onto montmorillonite from batch sorption and spectroscopic studies at increased ionic strength. Sci. Total Environ. 806, 150653.
Tournassat, C., Tinnacher, R.M., Grangeon, S., Davis, J.A., 2018. Modeling uranium(VI) adsorption onto montmorillonite under varying carbonate concentrations: a surface complexation model accounting for the spillover effect on surface potential. Geochim. Cosmochim. Acta 220, 291–308.
Trabelsi, R., Zouari, K., Araguás Araguás, L.J., Moulla, A.S., Sidibe, A.M., Bacar, T., 2024. Assessment of geochemical processes in the shared groundwater resources of the Taoudeni aquifer system (Sahel region, Africa). Hydrogeol. J. 32, 167–188.
Tullborg, E.L., Suksi, J., Geipel, G., Krall, L., Auque, L., Gimeno, M., Puigdomènech, I., 2017. The occurrences of $Ca_2UO_2(CO_3)_3$ complex in Fe(II) containing deep groundwater at Forsmark, eastern Sweden. Proc. Earth Planet. Sci. 17, 440–443.
van der Lee, J., De Windt, L., Lagneau, V., Goblet, P., 2002. Presentation and application of the reactive transport code HYTEC. In: Developments in Water Science, Vol. 47, pp. 599–606.
van der Lee, J., De Windt, L., Lagneau, Goblet, P., 2003. Module-oriented modeling of reactive transport with HYTEC. Comput. Geosci. 29, 265–275.
Wang, Z.M., Zachara, J.M., Yantasee, W., Gassman, P.L., Liu, C.X., Joly, A.G., 2004. Cryogenic laser induced fluorescence characterization of U(VI) in Hanford vadose zone pore waters. Environ. Sci. Technol. 38, 5591–5597.
Wang, Z., Lee, S.W., Catalano, J.G., Lezama-Pacheco, J.S., Bargar, J.R., Tebo, B.M., Giammar, D.E., 2013. Adsorption of uranium (VI) to manganese oxides: X-ray absorption spectroscopy and surface complexation modeling. Environ. Sci. Technol. 47, 850–858.
World Health Organization, 2022. Guidelines for Drinking-Water Quality: Fourth Edition Incorporating the First and Second Addenda, Geneva (Switzerland).
Yang, B., Cui, D., Meng, T., Guo, H., Lian, G., 2023. Characteristics and influencing factors of uranium adsorption by sandstones outside an acid in situ leaching uranium mining area. Environ. Earth Sci. 82, 532.
Zachara, J.M., Cowan, C.E., Schmidt, R.L., Ainsworth, C.C., 1988. Chromate adsorption by kaolinite. Clay Clay Miner. 36, 317–326.
Zouari, K., Trabelsi, R., Araguás Araguás, L.L., Hussaini, S., Rabe, S., Alassane, A., 2024. Use of hydrochemical and isotopic tracers to investigate the groundwater quality and recharge processes of the shared Iullemeden aquifer system in the Sahel region (Western Africa). Hydrogeol. J. 32, 219–240.